

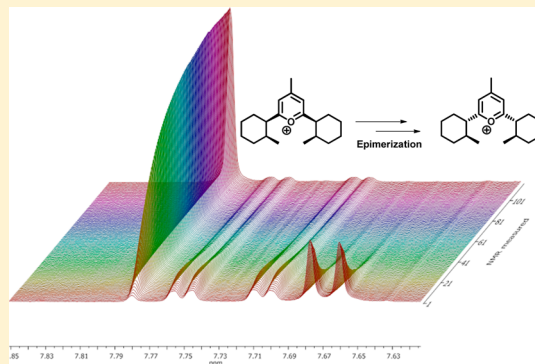
Kinetic Studies of the Epimerization of Diastereomeric Pirylium Salts

Nelson A. van der Velde, Holland T. Korbitz, Darrin J. Bellert, and Charles M. Garner*

Department of Chemistry and Biochemistry, Baylor University, Waco, Texas 76798, United States

S Supporting Information

ABSTRACT: Chiral pyrylium salts are almost unknown in the literature, and none that are epimerizable have been reported prior to our work. Herein, we report two new epimerizable pyryliums and the kinetics of the diastereomeric equilibration of these and one other example. All of these required a careful analysis of the ^1H NMR spectrum to identify the stereoisomers, particularly for one of them. The temporal evolution of the relative isomeric concentrations was determined through acquisition of progressive NMR spectra. The base-catalyzed isomerization kinetics were successfully modeled as sequential, pseudo-first-order reactions that transition through a long-lived intermediate. These results suggest that the pseudobase intermediate is the operative catalyst when epimerizations are initiated with amines with $\text{p}K_a$ 7.4 or greater. Given the bulky nature of the operative acid (pyrylium) and base (pseudobase), the rate of these epimerizations is sensitive to steric bulk in the pyrylium. Thus, the reaction kinetics slow by a factor of 25 when substituents are placed at the ortho versus para position on the pyrylium cyclohexane ring. This is likely due to the difficulty of pseudobase attack at the sterically crowded pyrylium acidic hydrogen position.



INTRODUCTION

Pyrylium salts (e.g., **1**) are precursors to a wide variety of heterocyclic systems, including pyridines, pyridiniums, thiopyryliums, and the relatively little-studied phosphinines (phosphabenzene).¹ In addition, carbon nucleophiles can convert pyryliums into benzene derivatives² and in some cases allow access to azulenes.^{3,4} This susceptibility to nucleophilic attack is the result of both the polarization and the limited aromaticity of the pyrylium ring; the latter has been estimated to be as low as 66% of that of benzene.⁵ Pyrylium salts have been incorporated as electron acceptors in electronic materials⁶ and near-IR dyes.⁷

Given the importance of pyrylium salts, it is striking that hardly any chiral pyryliums have been reported. Prior to our recent publication,⁸ we knew of only three chiral examples (Figure 1), one of which is the C_2 -asymmetric pyrylium recently reported⁹ by our group (**1**). Of the other two examples (**2**^{10,11} and **3**¹²), the former was racemic. Structure **2**, synthesized by Müller and co-workers, is the first example of an atropisomeric pyrylium, with the axial chirality induced by

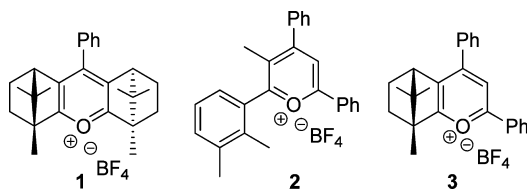


Figure 1. Previously reported chiral pyrylium salts.^{9–12}

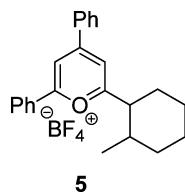
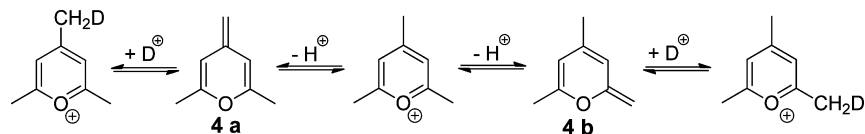
the pyrylium meta methyl group. One reason for this scarcity of chiral examples is that pyryliums are often involved as reaction intermediates rather than isolated and characterized materials. Another is that many pyrylium preparations tend to result in tar because of polymerization reactions.¹

Our interest in chiral pyryliums led us to investigate the configurational stability of chiral centers α to the pyrylium ring. Although no epimerizable (or even racemizable) pyryliums have been reported, deuterium exchange at ortho and especially para benzylic positions is well-known^{13–15} (Scheme 1). For example, in 2,4,6-trimethyl pyrylium, it was observed that both the 2/6-methyl (α) and 4-methyl (γ) hydrogens exchanged with D_2O , with the latter being faster by 1 order of magnitude.¹⁵ This proceeds via the pseudobase intermediates (e.g., **4a** and **4b**), which can be isolated sometimes.^{1,16} Detailed studies carried out by Williams¹⁷ on the hydrolysis of pyryliums found that the $\text{p}K_a$ of 2,4,6-trimethylpyrylium ion acting as a carbon acid in water was 6.7.

Because diastereomer ratios are easier to determine than enantiomer ratios, we sought to prepare pyryliums that would form diastereomers upon inversion at a benzylic center. We recently reported the synthesis of four new chiral asymmetric pyrylium salts,⁸ one of which (**5**, Figure 2) was suitable for epimerization studies. It was observed that pyrylium **5** was epimerized by catalytic amounts of *N*-methylmorpholine, converting an initial 39:61 cis/trans mixture to a 9:91 ratio at equilibrium. The synthesis of two new symmetrical, epimerizable

Received: July 25, 2013

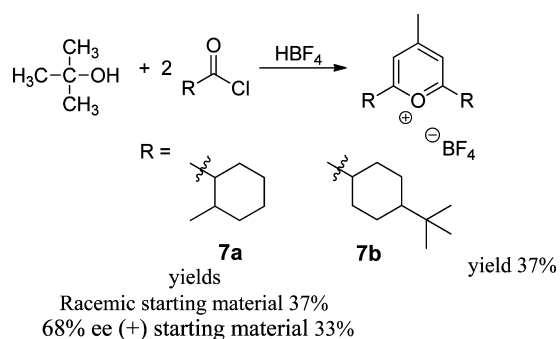
Published: October 31, 2013

Scheme 1. Mechanism of Methyl Deuteration by Isotopic Exchange with D₂OFigure 2. Pyrylium 5 previously synthesized by our group.⁸

able pyryliums and the first study of the base-catalyzed epimerization reaction kinetics of chiral pyrylium salts are reported here.

RESULTS AND DISCUSSION

Synthesis of New Symmetric Pyrylium Salts. Symmetric pyrylium salts (Scheme 2) were obtained in moderate yields

Scheme 2. Synthesis of C₂-Symmetrical Pyryliums from *tert*-Butanol

from a one-pot reaction of *tert*-butanol and an acyl chloride, with ethereal tetrafluoroboric acid as a condensing agent.¹⁸ Addition of ether precipitated the compounds as white powders.

When optimizing the conditions, a model system was used that consisted of pivaloyl chloride and triflic acid to synthesize the known¹⁸ 2,6-di-*tert*-butyl-4-methyl pyrylium triflate in 41% yield. Switching the condensing agent to ethereal tetrafluoroboric acid improved the yield to 56%.¹⁹ The ¹³C NMR spectrum of the symmetric pyryliums displayed characteristic peaks further downfield (around 183 and 175 ppm) than the typical aromatic region, which are indicative of deshielded carbons atoms ortho and para to the oxygen in the aromatic pyrylium ring.

Pyrylium 7a was prepared from the commercially available 86:14 mixture of racemic *cis*/*trans* 2-methylcyclohexanecarboxylic acid, resulting in a complex mixture of all six possible diastereomers, as evident through ¹H NMR. To aid in the identification of the NMR resonances, the starting carboxylic acid was partially resolved through three crystallizations of the (*S*)-(-)- α -methylbenzylamine salt from hexanes/isopropanol. A 5.2:1 ratio (68% ee) of (+):(-) *cis*-2-methylcyclohexane carboxylic acid containing 2 to 3% of the *trans* isomer was obtained. Pyrylium made from this (+)-enriched acid should be

depleted in any diastereomers derived from the (-)-acid. The pyrylium (33% yield) was prepared utilizing the partially resolved carboxylic acid, and, as expected, variations in the ¹H NMR peak intensities were observed (Figure 3). This verified

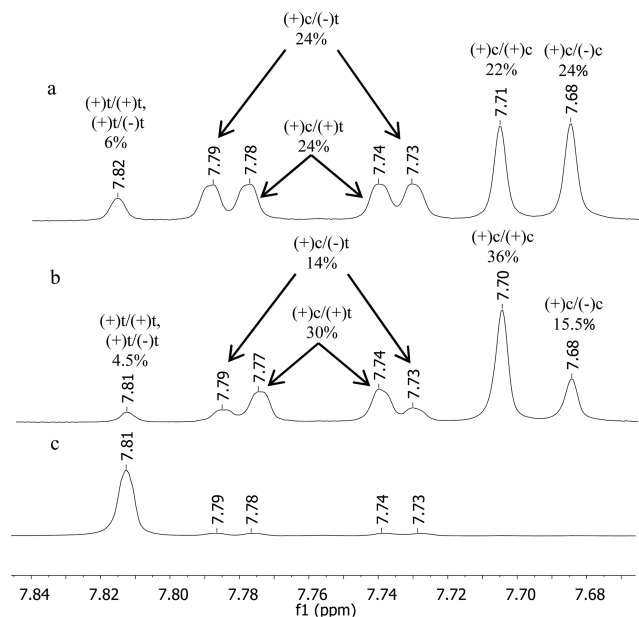


Figure 3. Partial ¹H NMR spectra of 7a. (a) Pyrylium obtained from racemic 2-methylcyclohexanecarboxylic acid (86% *cis*), (b) pyrylium obtained from 68% ee acid (97% *cis*), and (c) pyrylium after equilibration with 5 mol % *N*-methylmorpholine. t, *trans*; c, *cis*.

the presence of all six diastereomers, all but two of which exhibited separate aromatic signals. In the ¹H NMR spectrum for 7a, the presence of three symmetrical isomers (single peaks for both protons meta to oxygen) and two unsymmetrical isomers (two peaks for each proton meta to oxygen) were clearly observed. This information, combined with the results obtained from base-catalyzed epimerization of pyrylium 7a, presented below, provided sufficient evidence to determine the identity of each aromatic NMR resonance. As depicted in Figure 3a, the peak at $\delta = 7.81$ labeled (\pm)t/(\pm)t corresponds to the thermodynamically most stable stereoisomer, with the substituents in both rings *trans*. The symmetrical (+)-*trans*/(+)-*trans* and (+)-*trans*/(-)-*trans* diastereomers give a single aromatic resonance ($\delta = 7.81$) by coincidence. The resonances at $\delta = 7.79$ and 7.73 correspond to the unsymmetrical (+)-*cis*/(-)-*trans* diastereomer, labeled (+)c/(-)t. The resonances at $\delta = 7.77$ and 7.74 correspond to the unsymmetrical (+)-*cis*/(+)-*trans* diastereomer, labeled (+)c/(+)t. Note that for both unsymmetrical stereoisomers no coupling between the non-equivalent meta protons was resolved. The resonances at $\delta = 7.70$ and 7.68 correspond to the least stable symmetrical diastereomers (+)-*cis*/(+)-*cis* and (+)-*cis*/(-)-*cis*, respectively, labeled (+)c/(+)c and (+)c/(-)c. Note that the *cis*/*trans* ratio of the starting carboxylic acid has little effect on the diastereomer ratios in the pyrylium product. Epimerization is

clearly occurring during pyrylium synthesis, possibly at the acid chloride stage, but not in the pyrylium products, which were found to be entirely configurationally stable under neutral or acidic conditions.

Pyrylium **7b** was made from a 95:5 mixture of *trans*/*cis* isomers of 4-*tert*-butylcyclohexane carboxylic acid, resulting in a mixture of three diastereomers. From the meta protons in the aromatic region of the ^1H NMR spectrum for **7b** (Figure 4),

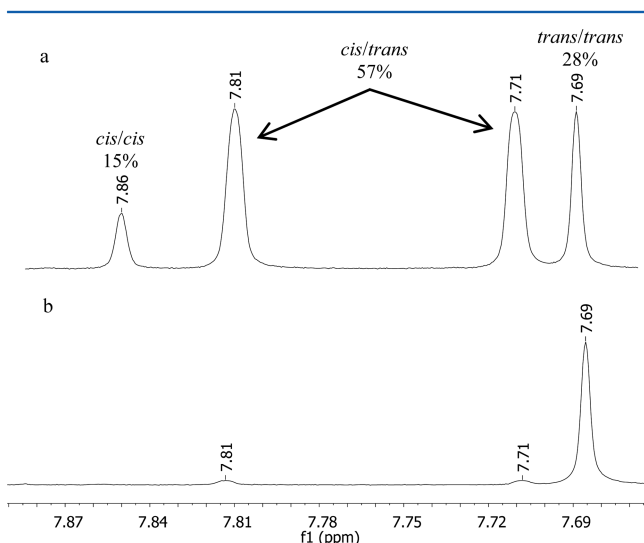


Figure 4. Partial ^1H NMR spectrum of **7b** (a) as-synthesized and (b) at equilibrium following the reaction with 5 mol % *N*-methylmorpholine.

the presence of two symmetrical isomers (single peak for both protons meta to oxygen) and one unsymmetrical isomer (two broader singlets for each proton meta to oxygen) were observed. Each stereoisomer was identified on the basis of the base-catalyzed epimerization of pyrylium **7b**. The most downfield peak (δ 7.86) corresponds to the least thermodynamically stable diastereomer (with substituents in both rings *cis* to each other). The unsymmetrical isomer with resonances at δ 7.81 and 7.71 has one ring *cis* and one *trans*. Unresolved coupling between the nonequivalent meta protons apparently results in broader peaks rather than resolved doublets. Finally, the thermodynamically most stable diastereomer (δ 7.69) with substituents in both rings *trans* to each other was easily identified upon equilibration. Again, epimerization was evident during the pyrylium synthesis, with about 43% of the rings being *cis* in the product, whereas the starting acid was only 5% *cis*.

Epimerization/Equilibration Studies. Although we had previously observed base-catalyzed epimerization of pyrylium

5,⁸ the stereochemical stability of the diastereomers under neutral conditions had not been established. Nonequilibrium mixtures of pyryliums **7a** and **7b** in CD_3CN were heated at 40 $^\circ\text{C}$ for 1 week without any detectable intensity changes in the ^1H NMR spectrum. Therefore, the pyryliums are configurationally stable in the absence of base. All of the subsequent epimerization measurements were performed at 25 $^\circ\text{C}$.

Optimization of the Experimental Conditions. To find appropriate base catalysts for the epimerization experiments, pyrylium **7a** in CDCl_3 was treated with 5 mol % of various amine bases covering a range of pK_a values: triethylamine (pK_a 10.8), *N*-methylmorpholine (pK_a 7.4), and pyridine (pK_a 5.1). Lesser quantities of base gave inconveniently slow equilibration times and larger amounts resulted in noticeable formation of pseudobase (**8**, Scheme 3) resonances in the NMR spectrum. The relative concentration of the *trans*/*trans* diastereomer over time in the presence of 5 mol % of these bases was plotted for comparison (Figure 5). Interestingly, although the weakly basic

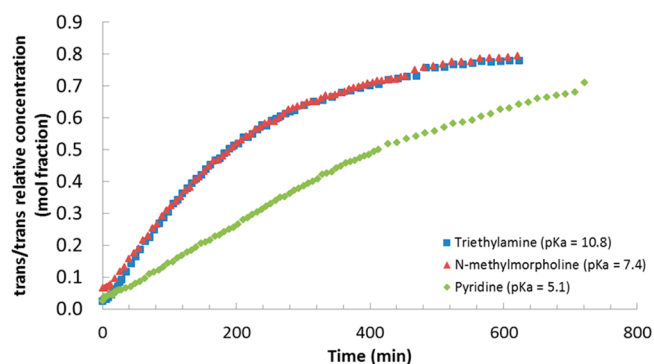
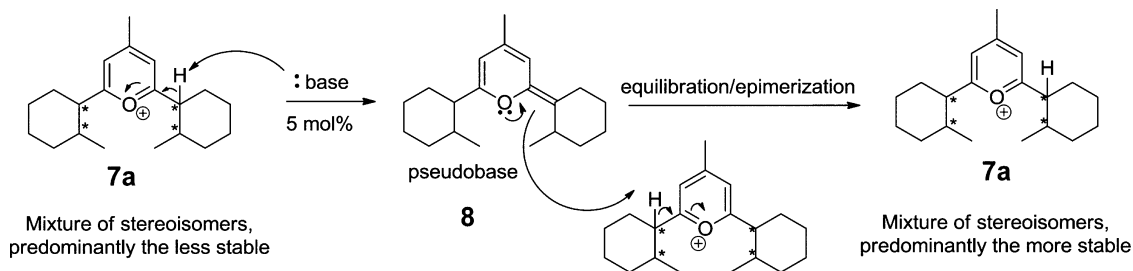


Figure 5. Equilibration rate of **7a** with 5 mol % of different bases.

pyridine gave slower reaction, triethylamine promoted equilibration at the same rate as *N*-methylmorpholine. This suggests that the conversion rate is independent of the base strength when the pK_a of the amine ≥ 7.4 . This is consistent with pyrylium serving as the operative acid (rather than the ammonium salt) and the pseudobase form serving as the base to drive the reaction to equilibrium as shown in Scheme 3. That is, the reactions are only *initiated* by a sufficiently basic amine and the thus formed pseudobase catalyzes the *cis*-to-*trans* conversion of the pyryliums.

Equilibration Experiments. Unsymmetrical pyrylium **5** (0.022 M) in CD_3CN at 25 $^\circ\text{C}$ was treated with a catalytic amount (5 mol %) of *N*-methylmorpholine, and ^1H NMR spectra were taken at progressive time intervals (Figure 6). Before the addition of base, two stereoisomers were present at a 39:61 *cis*/*trans* ratio. These stereoisomers were identified by

Scheme 3. Proposed Pyrylium Base-Catalyzed Equilibration Reaction Mechanism



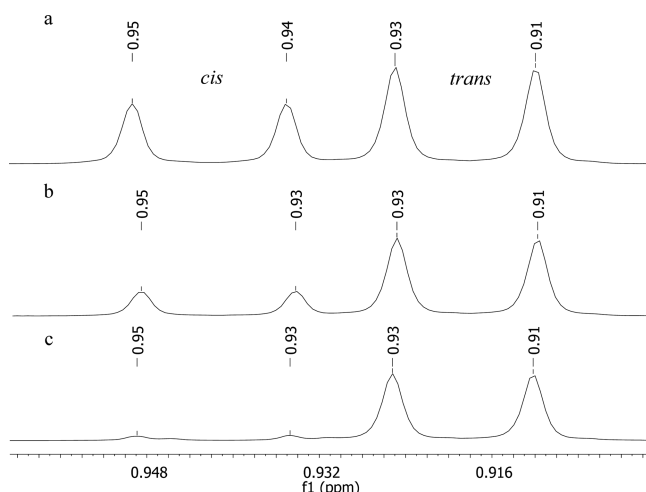


Figure 6. Partial ^1H NMR spectra of the equilibration reaction of **5** following the addition of 5 mol % *N*-methylmorpholine at times (a) 0, (b) 6, and (c) 119 min (equilibrium).

two sets of methyl doublets, the *cis* (δ 0.94, J = 7.2 Hz) and the *trans* (δ 0.92, J = 6.5 Hz) isomers. Intensity changes to these peaks caused by the addition of base were monitored (Figure 7). A gradual disappearance of the more downfield (*cis*, δ 0.94) doublet was noticed, whereas the integral of the more upfield (*trans*, δ 0.92) doublet increased. At equilibrium, the ratio of *cis/trans* isomers was 9:91. This equilibrium ratio is consistent with the known equatorial preference of the methyl group in methylcyclohexane (*cis/trans* 5:95).²⁰

Examining the first of the symmetrical pyryliums, pyrylium **7a** was studied in CDCl_3 solution because the resolution of the aromatic region was superior to that observed in CD_3CN . Pyrylium **7a** (0.022 M) in CDCl_3 at 25 °C was treated with 5 mol % of *N*-methylmorpholine. The ^1H NMR spectra were taken at progressive time intervals (Figure 3). For the analysis of the epimerization data, the (+)/(+) and (+)/(−) diastereomers of any given *cis/trans* isomers were integrated together. It was observed (Figure 8) that when the *cis/cis* isomers were decreasing the *cis/trans* isomers increased until they reached a maximum level and then started to decline. This is consistent with the *cis/cis* isomers converting to *cis/trans*

isomers as an intermediate step before converting to the *trans/trans* isomer.

Subsequently, symmetrical pyrylium **7b** (0.022 M) in CD_3CN at 25 °C was treated with a catalytic amount (5 mol %) of *N*-methylmorpholine, and ^1H NMR spectra were taken at progressive time intervals (Figure 4). Just as with pyryliums **5** and **7a**, equilibration occurred to predominantly (87%) the *trans/trans* stereoisomer.

Reaction Kinetic Results. Time-varying concentrations for the base-catalyzed *cis*-to-*trans* isomerization reaction of pyrylium **5** and the *cis/cis*-to-*trans/trans* isomerization for pyryliums **7a** and **7b** were measured through peak integration of ^1H NMR spectra acquired consecutively at 3 min intervals. These are presented in Figures 7–9. These isomerization reactions, however, are not simple first- or second-order processes and thus the time-varying concentrations were modeled to extract the kinetic parameters.

Compound **5** is structurally simpler than pyryliums **7a** or **7b**, with the *cis* form directly converting into the *trans* form (Scheme 4) via the pseudobase intermediate. The temporal response in Figure 7 suggests that this decay is exponential. For **5**, the *cis* pyrylium peak intensities were initially fit (dashed lines, Figure 7) to a single-exponential function that decays to its equilibrium concentration (eq 1, $B = 0$). This model, however, underestimates the reaction rate at early times and overestimates the approach to equilibrium at longer times. The *cis*-to-*trans* isomerization reaction of pyrylium **5** was therefore refit as a biexponential function with the parameters A , B , k_1 , and k_2 determined through minimization of the squared residuals between the NMR integrated areas and those calculated from eq 1. The application of the A , B , $k_1 = (4.8 \pm 0.50) \times 10^{-3} \text{ s}^{-1}$, and $k_2 = (3.6 \pm 0.33) \times 10^{-4} \text{ s}^{-1}$ values (Table 1) to eq 1 results in the solid curves of Figure 7. The improved agreement between measurement and the biexponential treatment suggests that there is a fast and a slow process involved in this conversion. However, the unambiguous interpretation of the reaction dynamics is not possible because multiple scenarios could cause this biexponential behavior. Therefore, only the k_1 and k_2 phenomenological rate constants are reported (Table 1) for the *cis*-to-*trans* isomerization of compound **5**. Visual inspection of the quality of the fit suggests that the rate constants presented in Table 1 have a conservative $\pm 10\%$ uncertainty.

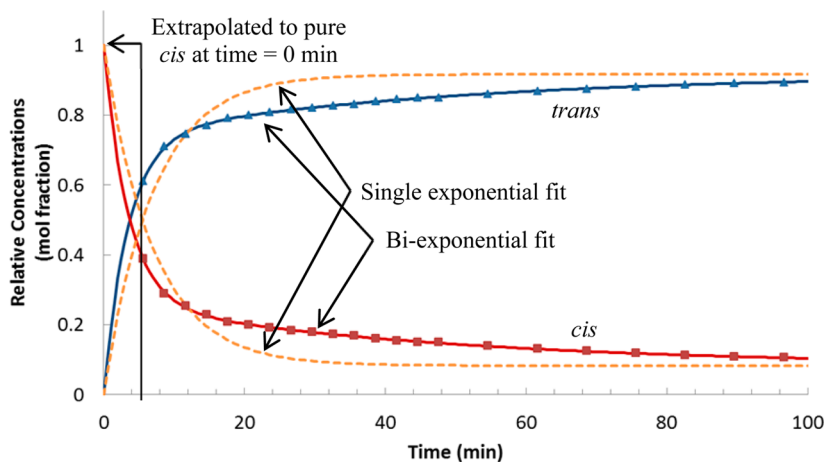


Figure 7. Base-catalyzed equilibration rate of pyrylium **5** (symbols) modeled using biexponential (solid curves) and single-exponential functions (dashed curves) in reaction with 5 mol % *N*-methylmorpholine. The modeled curve was obtained using eq 1.

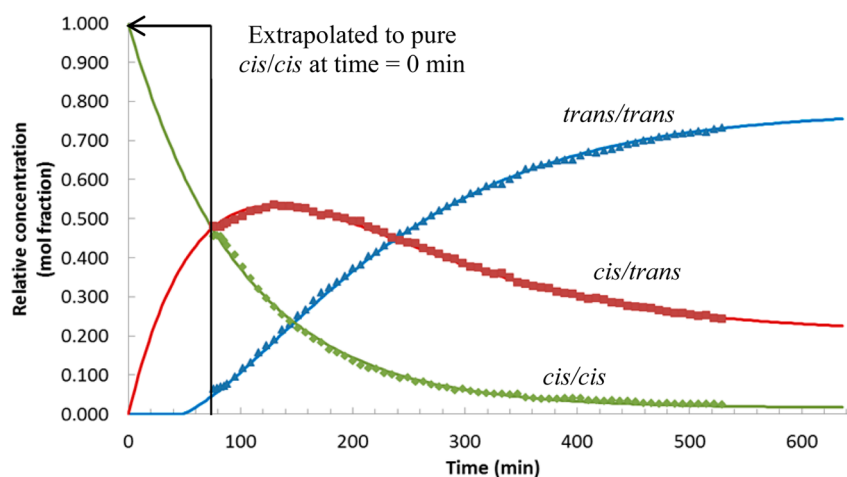
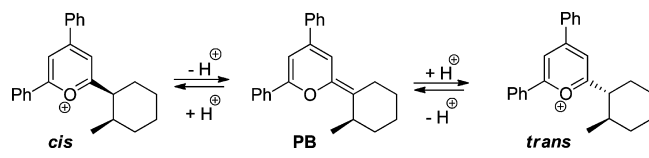


Figure 8. Measured relative concentrations (symbols) for the *N*-methylmorpholine-catalyzed isomerization reaction of pyrylium **7a**. Isomer concentrations were calculated (solid curves) from eqs 2–5 using the values recorded in Table 2.

Scheme 4. Proposed Base-Catalyzed Epimerization Mechanism for Pyrylium **5**



$$[\text{cis}]_t = Ae^{-k_1 t} + Be^{-k_2 t} + [\text{cis}]_{\text{eq}} \quad (1)$$

Analysis of ^1H NMR signals indicates that pyryliums **7a** and **7b** exist as three different geometric isomers (irrespective of \pm for **7a**). Integration of these spectral features provides the relative concentrations for the cis/cis, cis/trans, and trans/trans isomers of pyrylium **7a** and **7b** as the catalyzed reaction progresses in time. Figures 8 and 9 show that the cis/cis pyrylium isomer converts to the trans/trans form through a cis/trans intermediate structure, as shown in Scheme 5. Scheme 6 is a four-step kinetic mechanism that shows this conversion.

The systematic interconversion between the geometric isomers of pyryliums **7a** and **7b** are seen in Figures 8 and 9. Equations that predict this temporal development are sought from Scheme 6. Various assumptions are necessary to reduce this scheme to derive a set of differential equations that can be exactly integrated (detailed mathematical analysis is included in the Supporting Information). Although each step in Scheme 6 is in equilibrium, it must be assumed that the magnitudes of the rate constants k_1 and $k_4 \gg k_{-1}$ and k_{-4} such that the reverse reactions in steps 1 and 4 can be ignored. Furthermore, the pseudobase catalyst that is produced and consumed in the overall reaction is assumed constant such that its concentration can be incorporated into so-called pseudo-first-order rate constants. Finally, the cis pseudobase and trans pseudobase of Scheme 6, which are of insufficient concentration to be detected by NMR, are assumed to be in steady-state.

The application of these assumptions reduces the four-step mechanism to two steps and is shown as the net equation in Scheme 6. Here, k' and k'' are collections of the pseudo-first-order rate constants k_1 to k_4 . Moreover, this reduction associates the k' rate constant with the conversion of the cis/cis to cis/trans pyrylium isomer and the k'' with the cis/trans to trans/trans isomer. The temporal profiles of Figures 8 and 9 demonstrate the characteristics of simple sequential first-order reactions, in accord with the net reaction of Scheme 6. Here, the precursor decays into a long-lived intermediate with concentration that initially builds only to decay subsequently into a growing product. This scenario is fairly common to reaction kinetics, and the subsequent integration of the differential equations that result from the reduction of Scheme 6 yields eqs 2–5. Here, $[\text{cis/cis}]_0$ is the mol fraction of the cis/cis pyrylium isomer, and the calculations assumed pure cis/cis at time 0. However, the pyrylium salts were not obtained as single diastereomers; hence, the measurements do not begin at time 0 even though the curves in Figures 8 and 9 extend to that point.

$$[\text{cis/cis}]_t = [\text{cis/cis}]_0 e^{-k' t} + x \quad (2)$$

$$[\text{cis/trans}]_t = \frac{k'}{k'' - k'} [\text{cis/cis}]_0 (e^{-k' t} - e^{-k'' t}) + x \quad (3)$$

$$[\text{trans/trans}]_t = [\text{cis/cis}]_0 - [\text{cis/cis}]_t - [\text{cis/trans}]_t \quad (4)$$

$$x = [A]_{\text{eq}} - [A]_{\text{eq}} e^{-(k t)} \quad (5)$$

Equations 2–4 represent a model that describes the temporal development of the geometric pyrylium isomers. This model assumes complete conversion of the cis/cis to the trans/trans form for pyryliums **7a** and **7b**; however, complete conversion is not observed. Rather, the reaction equilibrates to a mixture of the geometric isomers at long times. This behavior is evident in Figures 8 and 9 as the geometric isomers asymptotically approach their relative equilibrium concentrations. This

Table 1. Pseudo-First-Order Rate Constants k_1 and k_2 (s^{-1}) and the Relative Equilibrium Concentrations for Pyrylium **5**^a

pyrylium	k_1 (s^{-1})	k_2 (s^{-1})	cis_{eq}^a	$\text{trans}_{\text{eq}}^a$
5	$(4.8 \pm 0.50) \times 10^{-3}$	$(3.6 \pm 0.33) \times 10^{-4}$	0.090 ± 0.01	0.91 ± 0.01

^amol fractions.

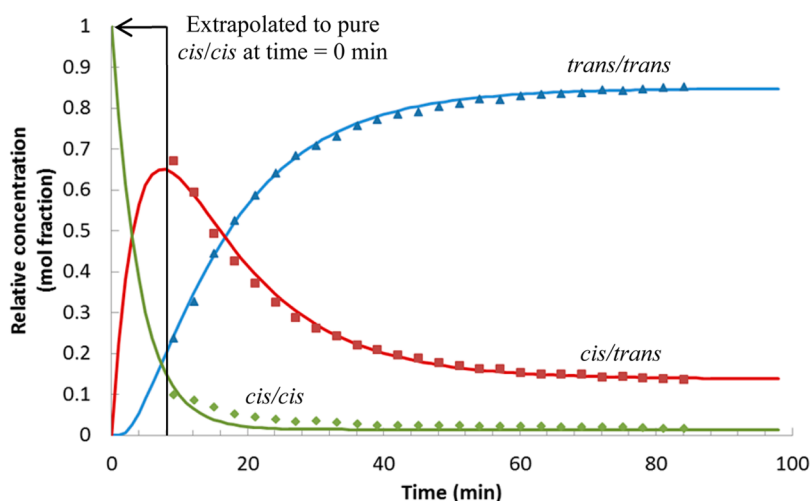
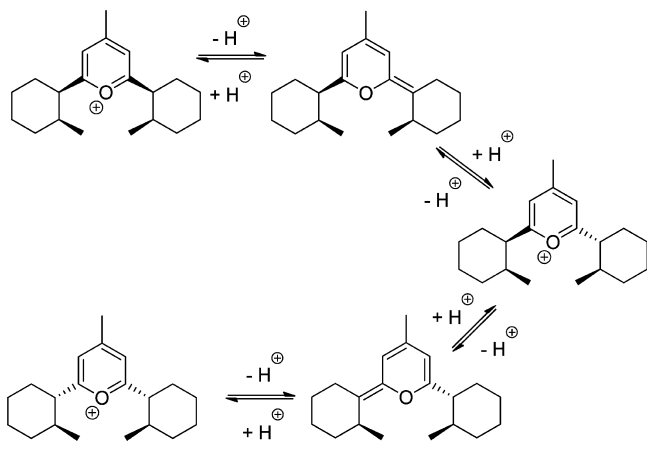


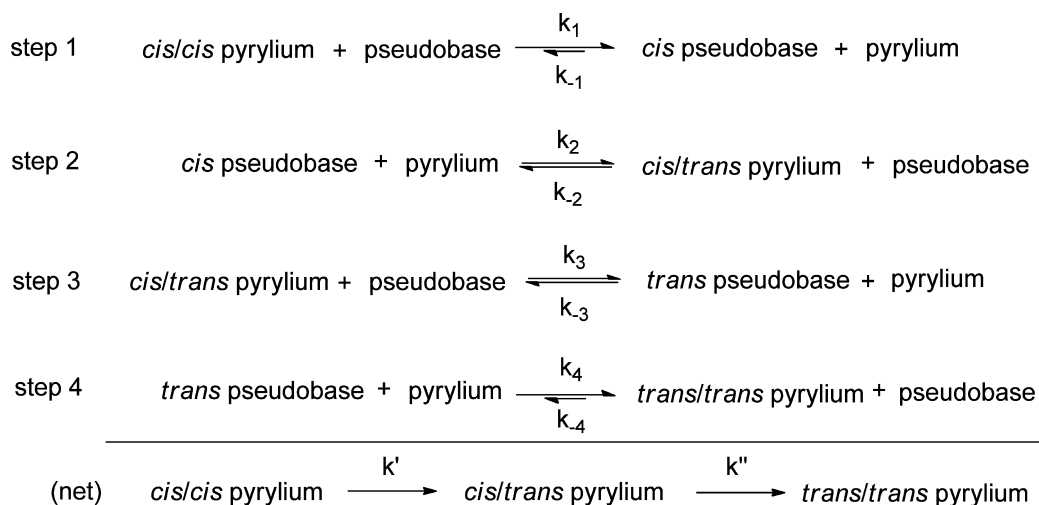
Figure 9. Measured relative concentrations (symbols) for the *N*-methylmorpholine-catalyzed isomerization reaction of pyrylium **7b**. Isomer concentrations were calculated (solid curves) from eqs 2–5 using the values recorded in Table 2.

Scheme 5. Proposed Base-Catalyzed Epimerization Mechanism for Pyrylium **7a**



asymptotic behavior is introduced into the model by including eq 5 as an additive term to eqs 2 and 3. Here, $[A]_{\text{eq}}$ is either the equilibrium concentration of *cis/cis* or the *cis/trans* isomer and $k = k'$ or k'' as when used in eqs 2 or 3, respectively.

Scheme 6. Proposed Reaction Mechanism for Pyryliums **7a** and **7b**



The model given by eqs 2–5 assumes that at time = 0, $[\textit{cis/cis}]_0 = 1$ and $[\textit{cis/trans}]_0 = [\textit{trans/trans}]_0 = 0$. However, the pyryliums were employed as mixtures of diastereomers, and the first ^1H NMR measurements in Figures 8 and 9 show appreciable concentrations of each isomer present. Indeed, it appears that the first measurements are made at 75 and 10 min for pyrylium **7a** and **7b**, respectively, following the initiation of the isomerization reaction. However, this is not due to the physical time delay between adding base and that required to make the first ^1H NMR measurement. Rather, our synthetic route generates a nonequilibrium mixture of pyrylium diastereomers, but this has no significant impact on the presented results.

Application of this model to the time-varying isomeric concentrations evident in Figures 8 and 9 is accomplished by minimizing the squared residuals between the observed ^1H NMR integrated areas and those calculated using eqs 2–5. An optimizer function in a commercially available spreadsheet package (Corel Quattro Pro 8.0) was used to minimize the sum of the squared residuals to the fit. The equilibrium concentrations of each isomer was held constant at the observed values and used as input values into the fit. The

Table 2. Pseudo-First-Order Rate Constants k' and k'' (s^{-1}) and the Relative Equilibrium Concentrations of Piryliums **7a** and **7b**^a

pyrylium	k' (s^{-1})	k'' (s^{-1})	(cis/cis) _{eq} ^a	(cis/trans) _{eq} ^a	(trans/trans) _{eq} ^a
7a	$(1.7 \pm 0.083) \times 10^{-4}$	$(1.4 \pm 0.067) \times 10^{-4}$	0.022 ± 0.005	0.21 ± 0.01	0.77 ± 0.01
7b	$(4.2 \pm 0.83) \times 10^{-3}$	$(1.25 \pm 0.25) \times 10^{-3}$	0.024 ± 0.005	0.14 ± 0.01	0.84 ± 0.01

^amol fractions.

pseudo-first-order rate constants k' and k'' were the only adjustable parameters in the model (under the constraint that $[\text{cis}/\text{cis}]_0 = 1$). The optimized values for k' and k'' that describe the isomerization kinetics for pyryliums **7a** and **7b** are provided in Table 2. The solid curves in Figures 8 and 9 are generated from the optimized rate constant values and the time-varying concentrations predicted by eqs 2–5. The nearly indistinguishable agreement between measurement (symbols) and calculation (solid curves) is indicative of the quality of the model in describing the interchange kinetics between the isomeric forms of pyryliums **7a** and **7b**.

Figure 8 shows the temporal evolution of the base-catalyzed epimerization of pyrylium **7a**. This is the slowest reaction in this study and requires times greater than 10 h for equilibration to occur. The curve suggests an induction period of roughly 50 min because no trans/trans product is produced during this time. The pseudo-first-order rate constants extracted from this fit are $k' = (1.7 \pm 0.083) \times 10^{-4} s^{-1}$ and $k'' = (1.4 \pm 0.067) \times 10^{-4} s^{-1}$ (Table 2). Figure 9 shows the time-varying concentrations of the base-catalyzed isomerization of pyrylium **7b**. This relatively fast reaction shows greater deviation from the proposed model than does the isomerization of pyrylium **7a**. This is particularly evident at early times (Figure 9). It is possible that the simplifying assumptions (constant pseudobase concentration, ignoring certain reverse reactions) that lead to the reduction of scheme six are more appropriate at longer times. It is also possible that the initial reaction between the pyrylium and pseudobase is not well-described by the model. It is clear that there is a fast component in the isomerization reaction of pyrylium **5** ($k = 4.8 \times 10^{-3}$) and it is possible that similarly fast reactions that occur in the initial interaction between pyrylium **7b** with pseudobase result in such early deviations with the model. The cause of this remains unclear. Visual inspection of the fit quality suggests that the rate constants for the faster reaction of pyrylium **7b** have conservative $\pm 20\%$ uncertainties. The agreement between the model and the base catalyzed isomerization of pyrylium **7a** is far superior (Figure 8) and the resulting uncertainty in the rate constants is placed at $\pm 5\%$ (Table 2).

Comparisons between the rate constants extracted from the fits relate to the different structural characteristics of pyrylium salts that affect the base-catalyzed epimerization rates. The primary difference between pyryliums **7a** and **7b** is in the location of the substituent on the cyclohexane ring. The substituent is ortho to the acidic hydrogen in pyrylium **7a**, whereas it is para in pyrylium **7b**. This results in k' and k'' rate constants that are 25 and 10 times smaller, respectively, in the base-catalyzed cis/cis-to-trans/trans isomerization of pyrylium **7a** when compared to **7b**. We believe that steric crowding of the reaction center imposed by substitution ortho to the benzylic proton slows the isomerization reaction. This effect is compounded by the formation of the carbon/carbon double bond in the pseudobase and the subsequent hindered rotation of the cyclohexane ring. Unable to rotate freely about this bond

locks the pyrylium **7a** pseudobase into a sterically hindered conformation.

CONCLUSION

Two new symmetric epimerizable pyrylium salts, one of them chiral, have been synthesized and characterized by ¹H NMR spectroscopy. To characterize the mixtures, it was necessary to compare spectra of the equilibrated products. In the case of pyrylium **7a**, it was also necessary to synthesize the pyrylium from partially resolved starting material (carboxylic acid) to aid in assigning the stereoisomers. This study presents the first kinetic analysis of the base-catalyzed epimerization of chiral pyrylium salts. A kinetic model based on sequential first-order reactions was developed that accounts for the temporal evolution of the isomeric concentrations of pyryliums **7a** and **7b**. Interestingly, the equilibration reaction of para-substituted **7b** is 25 times faster than ortho-substituted **7a**. Given the bulky nature of the operative acid (pyrylium) and base (pseudobase), it is not surprising that the rate of these reactions is sensitive to steric bulk near the epimerizable center. The extent to which epimerization impacts synthetic transformations (e.g., during conversion of α -chiral pyryliums to pyridines and phosphinines) remains to be determined.

EXPERIMENTAL SECTION

General Information. 2-Methylcyclohexane carboxylic acid was an 86:14 mixture of cis and trans isomers, respectively, based on NMR analysis and literature precedent.²¹ Hexanes, ethyl acetate, and methylene chloride were distilled prior to use. NMR spectra were obtained at 500 MHz for ¹H and 126 MHz for ¹³C. Spectra obtained in CDCl₃ were referenced to TMS (0 ppm) for ¹H and to CDCl₃ (77.16 ppm) for ¹³C. Spectra obtained in CD₃CN were referenced to solvent at 1.94 ppm for ¹H and 118.26 ppm for ¹³C. Mass spectrometry was carried out under positive ESI (electrospray ionization) using a Thermo Scientific LTQ Orbitrap Discovery instrument.

Partial Resolution of cis-2-Methylcyclohexanecarboxylic Acid. To 5.520 g (38.8 mmol) of commercial carboxylic acid that was an 86:14 mixture of cis/trans isomers by ¹H NMR [cis = 0.97 ppm (d, $J = 8.2$ Hz), trans = 0.94 ppm (d, $J = 6.5$ Hz)] dissolved in 50 mL of hexanes was cautiously added 5.00 mL (38.8 mmol) of (S)-(-)- α -methylbenzylamine. The resulting precipitate was heated at 60–65 °C, and isopropanol was slowly added with swirling until the solid was just dissolved. Upon slow cooling, fine needles formed that trapped the free solvent; however, vigorous shaking broke up the solid and allowed for filtration on a coarse frit. After washing with hexanes and drying under vacuum, the recrystallization procedure was repeated twice more by suspending the solid in hexanes (8 mL/g) and heating at 60–65 °C, and isopropanol was added until just dissolved. The enantiomer ratio was monitored by ¹H NMR of the salt (~10 mg in 0.7 mL of CDCl₃); chemical shifts were somewhat concentration-dependent, but the methyl doublet for the less soluble of the cis diastereomers was consistently downfield by about 0.015 ppm (0.877 vs 0.863 ppm) from the more soluble cis diastereomer. Because the center peaks of the cis diastereomers overlapped, integration of the outer peak of each doublet was used for quantitation. There were small amounts of the trans isomer also evident upfield (0.837 ppm), the diastereomers of which apparently gave coincident peaks. In this way, 2.250 g of a 5.2:1

ratio (68% ee) of the cis diastereomer containing 2–3% of the trans diastereomer was obtained. This was partitioned between 10 mL of 2 M HCl and dichloromethane, and the organic phase was dried with MgSO₄ and concentrated to give 1.140 g (8.03 mmol) of ~97% cis-(+)-2-methylcyclohexanecarboxylic acid. [α]_D²⁰ +3.2 (c 0.7, EtOAc); lit.²² [α]_D²¹ –8.0 (c 6.0, EtOH) for (1S,2R).

General Procedure for the Preparation of the Acyl Chlorides. One equivalent of the carboxylic acid and 1.5 equiv of oxalyl chloride were treated with a catalytic amount (3 μ L) of DMF and stirred for 1 h under nitrogen. Excess oxalyl chloride was then removed by rotary evaporation, and the product formation was confirmed by GC–MS. The compound was used without further purification.

General Procedure for the Preparation of the Pyrylium Salts 7a–b. One equivalent of *tert*-butanol, 4 equiv of acyl chloride, and 3 equiv of tetrafluoroboric acid diethyl etherate (51–57% HBF₄ in diethyl ether, 7.3 M) were heated at 85 °C for 2 h. The solution turned deep red. After cooling to room temperature, the reaction mixture was poured into approximately 40 mL of diethyl ether, precipitating the pyrylium salt.

2,6-Bis(2-methyl-cyclohexyl)-4-methyl-pyrylium Tetrafluoroborate (7a). From 0.17 mL (1.9 mmol) of *tert*-butanol, 1.270 g (8 mmol) of 2-methylcyclohexanoyl chloride, and 0.8 mL (5.8 mmol) of tetrafluoroboric acid diethyl etherate (51–57% HBF₄ in diethyl ether, 7.3 M), pyrylium 7a was obtained as white powder.

Pyrylium 7a from Racemic Starting Material. From 1.270 g (8 mmol) of 2-methylcyclohexanoyl chloride, the pyrylium was obtained as white powder (0.272 g, 0.73 mmol, 37% yield). mp 127–129 °C. ¹H NMR (500 MHz, CDCl₃) δ 7.81 (s, (+)-trans/(+)-trans and (+)-trans/(–)-trans diastereomers 7% of total), 7.79 (s, (+)-cis/(–)-trans diastereomer 24% of total), 7.77 (s, (+)-cis/(+)-trans diastereomer 26% of total), 7.74 (s, (+)-cis/(+)-trans diastereomer), 7.73 (s, (+)-cis/(–)-trans diastereomer), 7.70 (s, (+)-cis/(+)-cis diastereomer 21% of total), 7.68 (s, (+)-cis/(–)-cis diastereomer 22% of total). ¹³C NMR (126 MHz, CDCl₃) δ 183.5 (ortho-pyrylium), 183.4 (ortho-pyrylium), 183.30 (ortho-pyrylium), 183.27 (ortho-pyrylium), 183.25 (ortho-pyrylium), 183.2 (ortho-pyrylium), 175.4 (para-pyrylium), 175.3 (para-pyrylium), 174.74 (para-pyrylium), 174.72 (para-pyrylium), 123.2 (meta-pyrylium), 123.03 (meta-pyrylium), 123.00 (meta-pyrylium), 122.9 (meta-pyrylium), 122.6 (meta-pyrylium), 122.4 (meta-pyrylium), 51.7, 51.6, 46.5, 46.42, 46.37, 46.35, 36.62, 36.59, 36.5, 36.3, 34.7, 34.6, 33.51, 33.50, 33.49, 33.3, 32.6, 32.53, 32.52, 32.50, 32.2, 31.7, 25.66, 25.65, 25.63, 25.54, 25.47, 25.13, 25.11, 25.02, 24.98, 24.19, 24.13, 24.12, 22.3, 22.2, 20.6, 20.1, 19.91, 19.86, 14.0 (CH₃), 13.8 (CH₃), 13.7 (CH₃). HRMS *m/z* (ESI): calcd for C₂₀H₃₁O [M⁺], 287.2369; found, 287.2371.

Pyrylium 7a from Partially Resolved Starting Material. From 1.270 g (8 mmol) of 2-methylcyclohexanoyl chloride, the pyrylium was obtained as white powder (0.250 g, 0.67 mmol, 33% yield). ¹H NMR (500 MHz, CDCl₃) δ 7.81 (s, (+)-trans/(+)-trans and (+)-trans/(–)-trans diastereomers, 4.5% of total), 7.79 (s, (+)-cis/(–)-trans diastereomer, 14% of total), 7.77 (s, (+)-cis/(+)-trans diastereomer, 30% of total), 7.74 (s, (+)-cis/(+)-trans diastereomer), 7.73 (s, (+)-cis/(–)-trans diastereomer), 7.70 (s, (+)-cis/(+)-cis diastereomer, 36% of total), 7.68 (s, (+)-cis/(–)-cis diastereomer, 15.5% of total), 0.79 (d, *J* = 7.0 Hz), 0.78 (d, *J* = 7.1 Hz), 0.78 (d, *J* = 7.4 Hz). ¹³C NMR (126 MHz, CDCl₃) δ 183.4 (ortho-pyrylium), 183.4 (ortho-pyrylium), 183.3 (ortho-pyrylium), 175.2 (para-pyrylium), 174.6 (para-pyrylium), 123.0 (meta-pyrylium), 123.0 (meta-pyrylium), 122.6 (meta-pyrylium), 122.4 (meta-pyrylium), 51.8, 51.7, 46.6, 46.5, 46.4, 36.7, 36.3, 34.8, 33.5, 33.3, 32.61, 32.55, 32.5, 31.8, 25.7, 25.5, 25.2, 25.1, 25.0, 24.28, 24.25, 24.2, 22.5, 22.3, 22.2, 20.7, 20.1, 19.9, 19.7, 14.0, 13.9 (CH₃), 13.8 (CH₃), 13.8 (CH₃).

2,6-Bis(4-*tert*-butyl-cyclohexyl)-4-methyl-pyrylium Tetrafluoroborate (7b). From 0.11 mL (1.25 mmol) of *tert*-butanol, 1.002 g (4.9 mmol) of 4-*t*-butylcyclohexanoyl chloride, and 0.5 mL (3.65 mmol) of tetrafluoroboric acid diethyl etherate (51–57% HBF₄ in diethyl ether, 7.3 M), compound 7b obtained as white powder (0.241g, 0.53 mmol, 43% yield). mp 212–214 °C. ¹H NMR (500 MHz, CD₃CN) δ 7.86 (s, cis/cis stereoisomer 15% of total), 7.81 (s,

cis/trans stereoisomer, 57% of total), 7.71 (s, cis/trans stereoisomer), 7.69 (s, trans/trans stereoisomer, 28% of total), 2.71 (s, CH₃–Ar cis/cis stereoisomer), 2.68 (s, CH₃–Ar cis/trans stereoisomer), 2.66 (s, CH₃–Ar trans/trans stereoisomer), 0.902 (s, *t*-butyl cis/trans stereoisomer), 0.901 (s, *t*-butyl cis/trans stereoisomer), 0.83 (s, trans/trans), 0.81 (s, cis/cis stereoisomer). ¹³C NMR (126 MHz, CDCl₃) δ 183.7 (ortho-pyrylium), 183.6 (ortho-pyrylium), 183.5 (ortho-pyrylium), 183.2 (ortho-pyrylium), 175.7 (para-pyrylium), 175.1 (para-pyrylium), 174.2 (para-pyrylium), 123.1 (meta-pyrylium), 122.8 (meta-pyrylium), 121.9 (meta-pyrylium), 121.7 (meta-pyrylium), 47.82, 47.81, 47.12, 47.07, 43.8, 43.7, 39.1, 39.0, 32.7, 32.61, 32.57, 31.1, 31.0, 28.5, 28.3, 27.54 (*t*-butyl), 27.49 (*t*-butyl), 27.4 (*t*-butyl), 26.63, 26.61, 24.2, 24.14, 24.11, 23.71, 23.65. HRMS *m/z* (ESI): calcd for C₂₆H₄₃O [M⁺], 371.3308; found, 371.3310.

Epimerization Experiments. Base Solution Preparation. Stock solutions of triethylamine, *N*-methylmorpholine, and pyridine were prepared by dissolving 10 μ L of the amine in 990 μ L of the deuterated solvent, which was chosen for the best NMR resolution (CD₃CN for 5 and 7b and CDCl₃ for 7a). The concentration of the solutions were [triethylamine] = 0.072 M, [*N*-methylmorpholine] = 0.091 M, and [pyridine] = 0.124 M.

Base-Catalyzed Epimerization Experiments. All of the subsequent epimerization measurements were performed at 25 °C. The software package employed to model the data was Corel Quattro Pro 8.0.

Epimerization of 7a with Different Bases. A solution of 0.022 M of pyrylium 7a in CDCl₃ was prepared by dissolving 8 mg (0.022 mmol) in 990 μ L of the solvent in an NMR tube. Base (5 mol %, 0.0011 M) was added, either 16 μ L of the triethylamine stock solution, 12 μ L of the *N*-methylmorpholine stock solution, or 9 μ L of the pyridine stock solution, to the solution, and ¹H NMR was taken at progressive time intervals.

Epimerization of Pyryliums 5, 7a, and 7b with a 5 mol % Solution of *N*-Methylmorpholine. A solution of 0.022 M of pyrylium in deuterated solvent (CD₃CN or CDCl₃) was prepared by dissolving 8–10 mg (0.022 mmol) in 990 μ L of the solvent in an NMR tube. Then, 5 mol % of base (0.0011 M) was added to the solution, and ¹H NMR was taken at progressive time intervals at 25 °C. For pyrylium 5, 9 mg (0.022 mmol) of pyrylium was dissolved in CD₃CN and 13 μ L of the stock solution was added. For pyrylium 7a, 8 mg (0.022 mmol) of pyrylium was dissolved in CDCl₃ and 12 μ L of the stock solution was added. For pyrylium 7b, 10 mg (0.022 mmol) of pyrylium was dissolved in CD₃CN and 12 μ L of the stock solution was added.

■ ASSOCIATED CONTENT

● Supporting Information

Data obtained from the ¹H NMR kinetic experiments and from the mathematical model. ¹H NMR spectra for pyrylium 5 and for pyrylium 5 at equilibrium. ¹H NMR and ¹³C NMR spectra for novel compounds pyryliums 7a and 7b. This material is available free of charge via the Internet at <http://pubs.acs.org>.

■ AUTHOR INFORMATION

Corresponding Author

*E-mail: charles_garner@baylor.edu.

Notes

The authors declare no competing financial interest.

■ ACKNOWLEDGMENTS

We thank the Donors of the American Chemical Society Petroleum Research Fund (grant no. 47942-AC1) and the Robert A. Welch Foundation (grant no. AA-1395) for support of this work, the National Science Foundation (award no. CHE-0420802) for funding the purchase of our 500 MHz NMR, Dr. Alejandro Ramirez from the Mass Spectrometry Center at Baylor University for several analyses, and Katie Benjamin for all of the editing.

■ REFERENCES

- (1) Balaban, T. S., Balaban, A. T. *Houben–Weyl Methods of Molecular Transformations*; Thieme-Verlag: New York, 2004; Vol. 15, p 11.
- (2) Dimroth, K. *Angew. Chem.* **1960**, *72*, 331.
- (3) Hafner, K.; Kaiser, H. *Justus Liebigs Ann. Chem.* **1958**, *618*, 140.
- (4) Hafner, K.; Kaiser, H. *Org. Synth.* **1973**, 1088.
- (5) Bird, C. W. *Tetrahedron* **1986**, *42*, 89.
- (6) Byun, J.; Wie, J.; Seo, Y.; Kim, H.; Cho, S. *Res. J. Chem. Environ.* **2012**, *16*, 32.
- (7) Reynolds, G. A.; Drexhage, K. H. *J. Org. Chem.* **1977**, *42*, 885.
- (8) van der Velde, N. A.; Korbitz, H. T.; Garner, C. M. *Tetrahedron Lett.* **2012**, *53*, 5742.
- (9) Bell, J. R.; Franken, A.; Garner, C. M. *Tetrahedron* **2009**, *65*, 9368.
- (10) Muller, C.; Vogt, D. *Dalton Trans.* **2007**, 5505.
- (11) Muller, C.; Pidko, E. A.; Totev, D.; Lutz, M.; Spek, A. L.; van Santen, R. A.; Vogt, D. *Dalton Trans.* **2007**, 5372.
- (12) Barnaud, Y.; Maroni, P.; Simalty, M.; Madaule, Y. *Bull. Soc. Chim. Fr.* **1970**, *4*, 1398.
- (13) Stanoi, I.; Gard, E.; Uncuta, C.; Balaban, A. T. *Rev. Roum. Chim.* **1979**, *24*, 209.
- (14) Stanoi, I.; Gard, E.; Chiraleau, F.; Balaban, A. T. *Rev. Roum. Chim.* **1977**, *22*, 1359.
- (15) Gard, E.; Chiraleau, F.; Stanoi, I.; Balaban, A. T. *Rev. Roum. Chim.* **1973**, *18*, 257.
- (16) Katritzky, A. R.; Vassilatos, S. N.; Alajarin-Ceron, M. *Org. Magn. Reson.* **1983**, *21*, 587.
- (17) Williams, A. J. *Am. Chem. Soc.* **1971**, *93*, 2733.
- (18) Anderson, A. G.; Stang, P. J. *J. Org. Chem.* **1976**, *41*, 3034.
- (19) Doddi, G.; Ercolani, G. *Synth. Commun.* **1987**, *17*, 817.
- (20) Booth, H.; Everett, J. R. *J. Chem. Soc., Chem. Commun.* **1976**, 278.
- (21) Besson, M.; Delbecq, F.; Gallezot, P.; Neto, S.; Pinel, C. *Chem.—Eur. J.* **2000**, *6*, 949.
- (22) Oppolzer, W.; Kingma, A. J.; Poli, G. *Tetrahedron* **1989**, *45*, 479.